Synthesis and electrochemistry of novel heteronuclear Fe–Ru bi- and quatermetallocenes, conjugatively connected by ethene and thiophene bridges

Dagmar Obendorf [a,*], Herwig Schottenberger [b,*], Klaus Wurst [b], Norbert Schuler [b], Gerhard Laus [c,*]

[a] *Institute of Analytical Chemistry and Radiochemistry, University of Innsbruck, Innrain 52a, 6020 Innsbruck, Austria*
[b] *Institute of General, Inorganic and Theoretical Chemistry, University of Innsbruck, Innrain 52a, 6020 Innsbruck, Austria*
[c] *Immodal Pharmaka GmbH, Bundesstrasse 44, 6111 Volders, Austria*

Abstract

(*E*)-2-(1′-Formylruthenocenyl)ethenyl-1′,2,2′,3,3′,4,4′,5-octamethylferrocene (**1**) and (all-*E*)-2,5-bis[2-[1′-[2-(1′,2,2′,3,3′,4,4′,5-octamethylferrocenyl)ethenyl]ruthenocenyl]ethenyl]thiophene (**2**) were synthesized by a sequence of Wittig olefinations. The X-ray structure of **1** is reported. The cyclic voltammogram of compound **1** shows the irreversible one-electron transfer expected for ruthenocene and a reversible wave for the octamethylferrocene moiety. Both waves occur at about the same potential as observed for the parent metallocenes. Compound **2**, however, exhibits completely unusual redox properties. In contrast to most ruthenocene-containing compounds, a reversible two-electron transfer is observed at a significantly lower potential than found usually for ruthenocenes that can be attributed unambiguously to the independent oxidation/reduction of the two ruthenocene moieties. The unexpected stability of the oxidation products must be due to the presence of the thiophene–ethene bridge, which facilitates the oxidation reaction and stabilizes the reaction products by delocalization of the valence electrons.
© 2004 Elsevier B.V. All rights reserved.

Keywords: Metallocene; Cyclic voltammetry; Thiophene; Ferrocene; Ruthenocene

1. Introduction

Metallocenes have attracted continuous interest as electrophoric substituents in model systems [1] and, additionally, as redox- and charge-tuneable moieties in various application-relevant molecular composites [2]. In comparison to the well-developed chemistry of unsubstituted ferrocene with its numerous applications in organic synthesis, homogeneous catalysis, and materials science, the analogous chemistry of methylated ferrocene derivatives is rather limited. However, highly methylated ferrocenes are even more useful building blocks for advanced materials and molecular electronics with advantageous properties in comparison to normal ferrocene derivatives, since the presence of eight or nine methyl substituents leads to a significant decrease in oxidation potential, amplified donor capacity with correspondingly increased stability of the ferrocenium salts, and altered solubility [3]. Thus, the novel bimetallocene motifs introduced herein represent valuable models for tailor-made electrophoric molecular arrays, coulombic metal-metal interactions, and intervalence transfer

* Corresponding authors. Tel.: +43 512 507 5178; fax: +43 512 507 2965.

E-mail addresses: dagmar.obendorf@uibk.ac.at (D. Obendorf), herwig.schottenberger@uibk.ac.at (H. Schottenberger), gerhardlaus @hotmail.com (G. Laus).
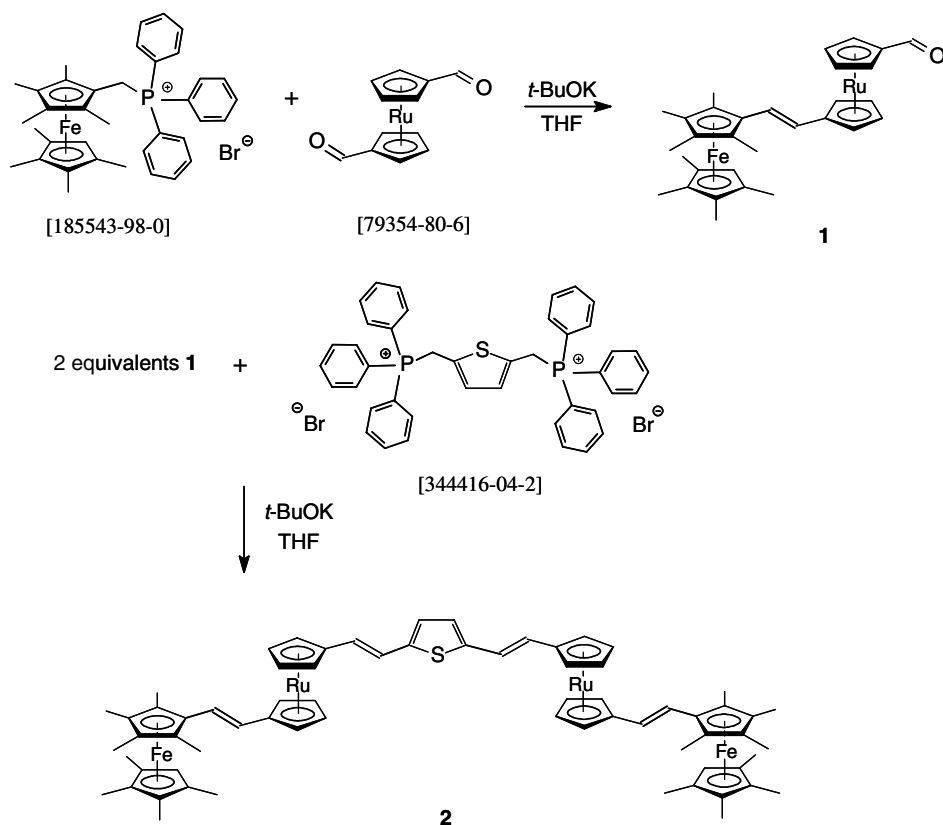
Scheme 1. Synthesis of bimetallocene **1** and quatermetallocene **2**.

phenomena [4], facilitated by the conjugated bridges [5]. These ethene bridges are conveniently introduced by Wittig sequences (Scheme 1) [6].

Electrochemical studies of the two title compounds, (E)-2-(1′-formylruthenocenyl)ethenyl-1′,2,2′,3,3′,4,4′, 5-octamethylferrocene (**1**) and (all-E)-2,5-bis[2-[1′-[2-(1′,2,2′,3,3′,4,4′,5-octamethylferrocenyl)ethenyl]ruthenocenyl]ethenyl]thiophene (**2**), should give more insight into electronic interactions, such as coulombic metal-metal interactions and intervalence transfer phenomena. Interaction and delocalization of the valence electrons is usually reflected in shifts of the redox potentials to higher or lower values compared to the values of the parent metallocenes and in changes in the degree of 'reversibility' of the redox reaction.

2. Results and discussion

2.1. Synthetic considerations

The underlying concept of synthesis of the desired conjugated symmetric quatermetallocene involves two subsequent Wittig reactions. In general, for a Wittig olefination two alternatives exist for the choice of aldehyde and phosphonium ylide. In terms of availability and economic viability of the required synthons, the following points were taken into consideration. For the

first step, the ylide precursor (1′,2,2′,3,3′,4,4′,5-octamethylferrocenyl)methyltriphenylphosphonium bromide is easy to prepare and purify [3], and the aldehyde component 1,1′-diformylruthenocene is available by a well described procedure [7]. In contrast, the inverse procedure requires 1,1′-diformyloctamethylferrocene, available only by a low-yield process [8], and yet undescribed ruthenocene-1,1′-diyl-bis(methyltriphenylphosphonium bromide) which would likely be cumbersome to prepare involving two additional steps (reduction of the dialdehyde, reaction with triphenylphosphine). From experience, side reactions are to be expected such as elimination of triphenylphosphine oxide on treatment of the salt with t-BuOK, ether formation by condensation of two molecules, or phenyl elimination [9]. In the second step, the strategy relies on the already described reactants yielding an aldehyde which, in turn, is to react with a symmetric diylide in a 2:1 ratio. The latter synthon is readily available from 2,5-bis(hydroxymethyl)thiophene [10] and triphenylphosphine hydrobromide. Otherwise, the intermediate **1** would have to be reduced and transformed to the corresponding methyltriphenylphosphonium bromide in order to react with 2,5-diformylthiophene. Therefore, the chosen first strategy is straight forward and gives an excellent yield of **2** (Scheme 1). It is noteworthy that no Z isomer of the bimetallocene **1** was isolated, and the final quatermetallocene **2** displayed all-E geometry as

indicated by the group of doubletts in the NMR spectrum with coupling constants of 16 Hz.

2.2. X-ray structure of 1

Single crystals of the intermediate (E)-2-(1′-formylruthenocenyl)ethenyl-1′,2,2′,3,3′,4,4′,5-octamethylferrocene (1) were obtained from the solution in CDCl$_3$ used for NMR spectroscopy. A 1:1 disordering of the formyl group is observed. The ferrocene subunit is nearly eclipsed with an average torsion angle of approximately 2°, whereas the ruthenocene subunit is slightly twisted with a torsion angle of 12°. The compound exhibits a 1,1′-conformation of the substituents on the ruthenocene moiety. The length of the C=C bond is 1.342 Å, and the Fec–C and Ruc–C bonds both are 1.462 Å long. The ethene bridge is rotated out of the plane of the ferrocene Cp ring by a dihedral angle of 20.0°, and out of the plane of the ruthenocene Cp ring by 18.9°. A plot of the molecular structure is shown in Fig. 1. Crystallographic details are given in Section 4.
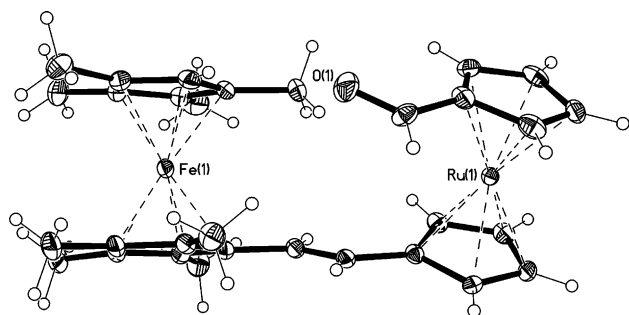

Fig. 1. ORTEP View of 1 drawn with 50% displacement ellipsoids.

2.3. Electrochemistry

The cyclovoltammogram of compound 1 shows two waves in the range between 0.4 and 1.5 V (Fig. 2). The reversible one-electron transfer at 90 mV can be easily attributed to the oxidation of the octamethylferrocene moiety, whereas the irreversible peak at 1.22 V must be due to the one-electron oxidation of ruthenocene (Table 1). Slight interaction between the two metallocene centers leads to a shift towards more positive oxidation potentials compared to the simple metallocenes (Table 2).The second irreversible wave at about 1.64
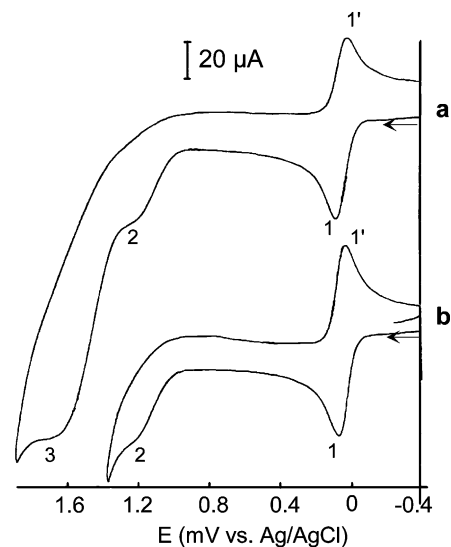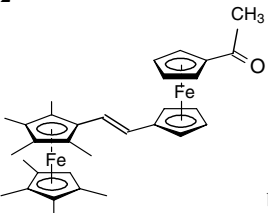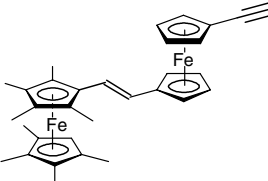

Fig. 2. Cyclic voltammograms for oxidation of 1 in CH$_3$CN, (a) potential range: −400 to 1800 mV; scan rate: 100 mV s^{-1}; $c = 0.35$ mmol/L (b) potential range: −400 to 1400 mV; scan rate: 50 mV s^{-1}.

Table 1
Electrochemical data[a] of compounds **1** and **2** and similar bimetallocenes

Compound	E_1^o/mV (ΔE_p/mV)	E_2^o/mV (ΔE_p/mV)	E_3^o/mV
1	90 (60)	1220 (irr 1e)	1640 (irr >2e)
2	40 (80) (2 × 1e)	600 (80) (2 × 1e)	1440 (irr 2e)
	90 (60)	780 (60)	
b	90 (60)	720 (60)	

[a] vs. Ag/AgCl.
[b] From [6].

Table 2
Electrochemical data of selected metallocenes, bi- and oligometallocenes

Compound	E_1^{o}/mV (ΔE_p/mV)	E_2^{o}/mV (ΔE_p/mV)	E_3^{o}/mV (ΔE_p/mV)	E_4^{o}/mV (ΔE_p/mV)
Ruthenocene	1040 (irr 2e)			
Ferrocene[a]	495 (80)			
Octamethylferrocene	60 (80)			
Decamethylferrocene[b]	1 (59)			
Bisfulvalene [Fe–Fe][c]	130 (60)	720 (60)		
Bisfulvalene [Ru–Co][+d]	−1750 (56)	−770 (61)	1450 (irr 1e)	
Biferrocene	310 (60)	640 (60)		
Diferrocenylethyne	625 (60)	753 (60)		
Terferrocene[c]	220 (60)	440 (60)	820 (60)	
1,1′-Diferrocenylcobaltocenium hexafluorophosphate[e]	−1930 (100)	−1050 (60)	550 (60)	670 (60)
1,1′-Dicobaltoceniumylruthenocene bishexafluorophosphate[e]	−1890 (100)	−990 (69)	−870 (60)	1440 (irr 2e)

  [a] Measured in $CH_3CN/CH_2Cl_2/12{:}1$; v:v); this paper.
  [b] From [25].
  [c] From [26].
  [d] From [17].
  [e] From [19,27].

V, with a peak height of about 2.5× the height of a reversible one-electron transfer, is most likely due to oxidation of the formyl group and the ethene bridge. Moreover, scanning to a more positive potential (>1.5 V) leads to beginning decomposition, which is indicated by a decreasing peak-current-ratio of peak 1/1′.

Interpretation of the cyclovoltammogram of compound **2** is not so straightforward (Fig. 3). Two reversible waves at 40 and 600 mV are observed, each corresponding to two 'reversible' one-electron transfers. The irreversible oxidation peak at 1.44 V has a peak height of about 50–65% of the first two waves. Comparing the redox potential of the first wave with the values for octamethylferrocene (Tables 1 and 2) it can be easily attributed to the reversible one-electron oxidation/reduction of the octamethylferrocene moiety. In this case, interaction between the adjacent metallocene centers leads to a shift of 60 mV towards more negative oxidation potentials compared to the simple metallocenes. The peak height of the wave at 40 mV is almost exactly twice the height of a reversible one-electron transfer as could be estimated by comparing the peak height found with the theoretical peak current calculated from the Randles–Sevcik equation according to

$$i_p = nFAD^{1/2}C^* \left(\frac{nF}{RT}\right)^{1/2} v^{1/2} 0.4463$$

(assuming a diffusion constant

D of 1×10^{-5} cm^2 s^{-1}).

Such a behavior would be expected whenever two identical redox-centers become electronically independent due to the distance between them. That means that the $\Delta E^o = E_2^o - E_1^o$ between the first and the second electron transfer arises purely from statistical reasons, that is $\Delta E^o = (-)2RT \ln 2 = (-)35.6$ mV [11]. Under these conditions, the observed wave has all characteristics of
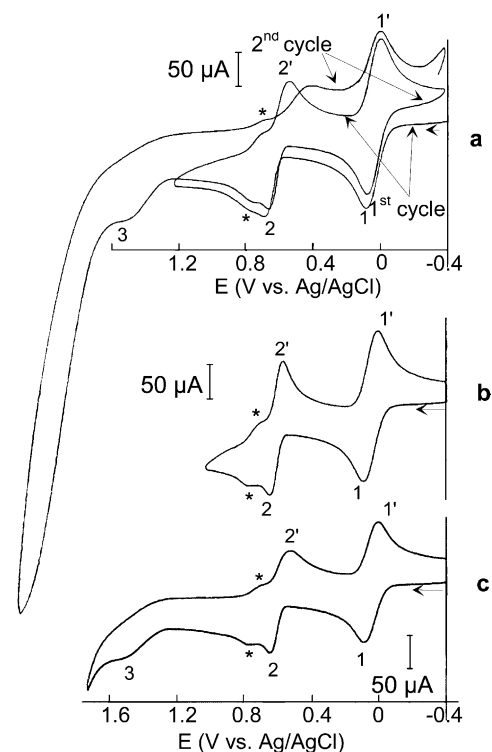

Fig. 3. Cyclic voltammograms for oxidation of **2** in CH_3CN/CH_2Cl_2 (12:1, v:v), (a) potential range: −400 to 2000 mV, scan rate: 100 mV s^{-1}, c = 0.35 mmol/L; (b) potential range: −400 to 1000 mV, scan rate: 100 mV s^{-1}; (c) potential range: −400 to 1800 mV, scan rate: 50 mV s^{-1}.

a one-electron transfer, though it is actually the result of two merged one-electron waves with a peak height of exactly twice that of a one-electron transfer. This same concept can be extended to the oxidation/reduction of molecules containing n equivalent, non-interacting redox active centers [12].

However, a single overall two-electron oxidation/ reduction peak would also be obtained in case of "potential inversion" of the redox potentials. Here, in contrast to the normal situation removal/introduction of the second electron occurs with greater ease than the first reaction. Thus, in case of an oxidation E_2^o is less positive than E_1^o. In most cases, potential inversion is due to a significant structural change associated with the first and/or the second electron-transfer reaction. Examples of potential inversion have been reviewed and cited in recent literature [13]. Though at first sight it did not seem very likely that potential inversion occurs in case of compound **2** it had to be taken into account. Further information as to the possible extent of potential inversion was expected from digital simulations (see below).

Identification of the redox processes leading to the second reversible wave 2/2′ and the third irreversible wave 3 is not free from ambiguity. The redox potential of ruthenocenes usually lies in the range between 1.0 and 1.5 V (vs. Ag/AgCl) (Table 2) and the oxidation of thiophene derivatives generally also occurs at rather high potential in acetonitrile (at about 1.8 V) [14,15]. The resulting oxidation products are usually very reactive, and only in the case of thiophene polymers reversible redox behavior is observed. On the other hand, the peak current of 2/2′ is closer to two simultaneous one-electron transfer waves similar to the wave attributed to the ferrocene moieties, which could be explained rather by an independent one-electron oxidation of the two ruthenocene centers than by a reversible 2-electron oxidation of thiophene. Thus, it seems to be more plausible to attribute wave 2/2′ to the reversible oxidation of the two ruthenocene moieties and wave 3 to the irreversible two-electron oxidation of thiophene. It seems that the presence of the thiophene bridge facilitates oxidation and stabilizes the oxidation products, since all redox potentials are shifted to lower potential values compared to the parent molecules. The thiophene bridge and the ruthenocene moiety are more strongly affected (the potential shift is about 0.4 V) than the ferrocene groups. The reaction products seem to be sufficiently stable, and only at potentials >1.8 V subsequent chemical reactions lead to decomposition of the molecule. This is clearly demonstrated by the decreasing reversibility of wave 2/2′ (Fig. 3(a)) after a scan to potentials higher than 1.8 V. However, the shoulder (marked by an asterisk in Fig. 3) at about 740/680 mV might be caused by an impurity or by adsorption of the compound as well as further oxidation of reaction products formed after the first electron transfer at the ruthenocene moieties.

In order to get further support of the postulated redox mechanism digital simulations using the software DigiSim 3.03 (BioanalyticalSystems) were performed. The most satisfactory result is demonstrated in Fig. 4, the simulation data are given in the figure caption. It has to be noted, however, that the cyclovoltammograms
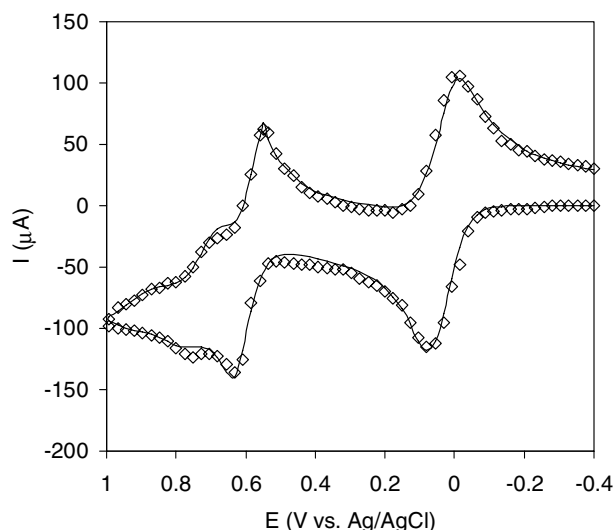

Fig. 4. Superposition of simulated (solid line) and experimental ($\diamond$) voltammogram: potential range: -400 to 1000 mV; scan rate: 100 mV s^{-1}; $c = 0.35$ mmol/L; electrode geometry = planar, area = 0.669 cm^2; simulation parameter values: all diffusion coefficients set equal to 1.06×10^{-5} cm^2 s^{-1} and $\alpha = 0.5$; residual resistance $R = 100$ Ω; ferrocene moieties: $E_1^o = 0.033$ V, $k_{s1} = 2$ cm s^{-1}; $E_2^o = 0.078$ V, $k_{s2} = 2$ cm s^{-1}; ruthenocene moieties: $E_3^o = 0.62$ V, $k_{s3} = 5 \times 10^{-2}$ cm s^{-1}; $E_4^o = 0.64$ V, $k_{s4} = 1.9 \times 10^{-3}$ cm s^{-1}; chemical reaction: $K_{eq\,Ru1} = 1.7$; $k_{f\,Ru1} = 0.69$; $K_{eq\,Ru2} = 0.27$; $k_{f\,Ru2} = 6.1$; oxidation of the reaction products: $E_5^o = 0.73$ V, $k_{s5} = 8.7 \times 10^{-3}$ cm s^{-1}; $E_6^o = 0.94$ V, $k_{s6} = 1.2 \times 10^{-2}$ cm s^{-1}.

had been recorded on an analogue XY-recorder and were manually converted into current–potential couples. In this manner, only a very low resolution of the experimental cyclovoltammogram could be obtained, which did not allow exact fitting of simulated and experimental data. Nonetheless, informations supporting the assumptions given above can be derived from the simulations. First of all, oxidation of the two ferrocene moieties is reversible and occurs according to a so-called "statistical" two-electron transfer with a ΔE^o of about 35 mV and there is no potential inversion. Also, the first quasi-reversible oxidation of the ruthenocene moieties occurs according to a normal order of potential, though E_3^o and E_4^o are somewhat closer than the potentials found for the ferrocene units. According to the simulation data, it seems to be most likely that oxidation of each ruthenocene unit follows an ECE-mechanism. A relatively slow chemical reaction after the first one-electron transfer, most probably a structural rearrangement leading to fulvenoid structures as discussed for other ethene-linked ruthenocenes [16], is followed by further quasireversible one-electron oxidations of the reaction products. In this case the reaction product of the first ruthenocene moiety is oxidized at a higher potential (E_6^o) than the reaction product of the second ruthenocene (E_5^o). These oxidations give rise to the shoulders observed in the experimental cyclovoltammogram.

The redox behavior of compound **2** is completely unexpected and in contrast to the data found for most ruthenocenes (see Table 2). In almost all cases irreversible one- or two-electron oxidations are reported. Only recently, the electrochemistry of some ethene-bridged ruthenocene compounds was published [16], which appeared to be very similar to the data obtained for compound **2**.

3. Conclusions

Non-conjugatively bridged ruthenocenylmetallocene systems have been previously shown [17,18] to exhibit the typical electrochemical behavior of separate metallocene fragments (apart from shifts to more positive potential due to coulombic interaction between the two linked metallocene centers): a reversible one-electron transfer for ferrocene (and cobaltocene), and an irreversible one- or two-electron transfer for ruthenocene. However, the same behavior has been observed also in cases of conjugatively bridged oligometallocenes with varying conjugation lengths [19]. Thus, other or additional structural criteria have to be considered in order to explain the rare cases of deviating electrochemical behavior of bridged ruthenocenylmetallocenes [16, this paper]. One explanation for the surprising reversibility of the ruthenocene oxidation might be the ability of the molecule to adopt fulvenoid resonance structures, which are implicated also in spin-pairing phenomena as well as in the electronic stabilisation of oxidized binickelocene systems [20–23]. It remains to be verified if the presence of two ruthenocene units is necessary and sufficient for the unique electrochemical behavior, or if the vicinity of an easily oxidizable metallocene like ferrocene (which is also capable of a cooperative fulvenoid resonance contribution) [24] could be operative as well. As a consequence, new model compounds will have to be designed for further electrochemical studies.

4. Experimental

4.1. Instrumentation

Cyclic voltammetry experiments were carried out with a HEKA potentiostat–galvanostat PG 28 system using a platinum ring working electrode, a glassy carbon counter electrode, and an Ag/AgCl/KCl (Friscolyt, Ingold) reference electrode as described previously [19]. Solutions of the metallocenes were approximately 0.35 mM in acetonitrile (for **1**) or acetonitrile/dichloromethane (12:1, v:v; for **2**) and contained 0.1 M *n*-tetrabutylammonium hexafluorophosphate as supporting electrolyte. In this supporting electrolyte the ferrocene/

ferrocenium couple appears at 495 mV (see Table 2) with a somewhat larger peak separation of 80 mV compared to the value of 60 mV predicted for a reversible one-electron transfer. This can be explained by uncompensated solution resistance, which was also verified by including a solution resistance of 100 Ω in digital simulations. Simulations of cyclic voltammograms were performed using the software package DigiSim 3.03 (Bioanalytical Systems).

Diffraction data were collected on a Siemens P4 diffractometer with graphite-monochromated Mo Kα radiation ($\lambda = 71.073$ pm) via ω-scans and refined against F^2.

4.2. Synthesis and characterisation

4.2.1. (E)-2-(1'-formylruthenocenyl)ethenyl-1',2,2',3,3',-4,4',5-octamethylferrocene (**1**)

Potassium *t*-butoxide (0.189 g, 1.68 mmol) and (1',2,2',3,3',4,4',5-octamethylferrocenyl)methyltriphenylphosphonium bromide (1.000 g, 1.53 mmol) were added to dry tetrahydrofuran (30 mL) at −78 °C. The solution was stirred at 0 °C for 1 h and cooled again to −78 °C. 1,1'-diformylruthenocene (0.483 g, 1.68 mmol) was added, and the red solution was stirred for 2 h at room temperature. After removal of the solvent the residue was partitioned between water and diethyl ether. The organic phase was washed twice with water and dried over anhydrous Na$_2$SO$_4$. The crude product was purified by column chromatography (diethyl ether/*n*-hexane 1:1, slightly acidic alumina with 5% water; R_f 0.62) and vacuum-dried to give 0.622 g (70% of theoretical yield) **1** as a red powder with m.p. 82 °C. IR (KBr): ν 2966, 2946, 2900, 2856, 1679, 1630, 1455, 1422, 1375, 1262, 1245, 1027, 957, 820 cm^{-1}. ^{1}H NMR (CDCl$_3$, TMS): δ 1.50 (s, 6H), 1.61 (s, 6H), 1.71 (s, 6H), 1.81 (s, 6H), 3.33 (s, 1H), 4.65 (ps-t, 2H), 4.83 (ps-t, 2H), 4.89 (ps-t, 2H), 5.06 (ps-t, 2H), 6.15 (d, 1H, *J* 16.2 Hz), 6.38 (d, 1H, *J* 16.2 Hz), 9.69 (s, 1H) ppm. HRMS (EI): *m/z* 582.1151; calculated for C$_{31}$H$_{36}$FeRuO: 582.1159. UV–Vis (CH$_2$Cl$_2$): λ_{max} (log ε) 312 (4.27), 377 (3.76), 484 (3.56), 714 (3.76) nm.

4.2.2. Thiophene-2,5-diyl-bis(methylene)bis(triphenylphosphonium bromide) [344416-04-2]

To a solution of 2,5-bis(hydroxymethyl)thiophene (0.438 g, 3.04 mmol) in O$_2$-free acetonitrile (120 mL) was added triphenylphosphine hydrobromide (1.981 g, 5.77 mmol) all at once. The mixture was refluxed for 2 h. After cooling, the solvent was removed, and the residue was dissolved in chloroform (20 mL). The product was precipitated by addition of diethyl ether (150 mL). The white solid was filtered off and washed with diethyl ether (320 mL) and dried to yield 2.078 g (86% of theoretical yield) with m.p. 195–200 °C (dec.). IR (KBr) ν 3043, 2838, 2819, 1586, 1486, 1437, 1113, 996, 751,

743, 724, 718, 691, 523, 505 cm^{-1}. MS (FAB): *m/z* 713.5 ($C_{42}H_{36}^{79}BrP_2S$), 715.6 ($C_{42}H_{36}^{81}BrP_2S$).

4.2.3. (all-E)-2,5-bis[2-[1'-[2-(1',2,2',3,3',4,4',5-octamethylferrocenyl)ethenyl]ruthenocenyl]ethenyl]thiophene (2)

Potassium *t*-butoxide (0.064 g, 0.56 mmol) and thiophene-2,5-diyl-bis(methylene)bis(triphenylphosphonium bromide) (0.225 g, 0.28 mmol) were added to dry tetrahydrofuran (10 mL) at −78 °C. The suspension was stirred at 0 °C for 1 h and cooled again to −78 °C. Compound **1** (0.300 g, 0.52 mmol) was added, and the red solution was stirred for 2 h at room temperature. After removal of the solvent, the residue was partitioned between water and diethyl ether. The organic phase was washed twice with water and dried over anhydrous Na_2SO_4. The crude product was purified by column chromatography (diethyl ether/*n*-hexane 1:1, neutral alumina with 5% water; R_f 0.32) and vacuum-dried to give 0.326 g (94% of theoretical yield) **2** as a red powder with m.p. 46 °C. IR (KBr): *ν* 3087, 3058, 2966, 2945, 2858, 1634, 1378, 1028, 955, 940, 807 cm^{-1}. ^{1}H NMR (CDCl$_3$, TMS): δ 1.6–1.8 (m, 48 H), 3.29 (s, 2H), 4.5–4.6 (m, 8H), 4.8–4.8 (m, 8H), 6.0–6.8 (m, 10H) ppm. HRMS (FAB): *m/z* 1240.2439; calculated for $C_{68}H_{76}Fe_2Ru_2S$: 1240.2453. UV–Vis (CH$_2$Cl$_2$): λ_{max} (log ε) 256 (4.62), 311 (4.55), 401 (4.31) nm.

4.2.4. Crystal data of 1

Orange prism (0.35 × 0.35 × 0.25 mm) from CDCl$_3$, *M* = 581.52, triclinic, *a* = 884.3(2), *b* = 914.1(3), *c* = 1716.2(3) pm, α = 99.79(2), β = 95.60(2), γ = 106.91(2)°, *V* = 1.2920(6) nm^3, *T* = 213 K, space group $P\bar{1}$ (no. 2), *Z* = 2, μ = 1.167 mm^{-1}. 4859 reflections were measured, 4528 independent (R_{int}=0.0284), 4343 observed, R_1 = 0.0323 and wR_2 = 0.0777 ($I > 2\sigma I$)), R_1 = 0.0360 and wR_2 = 0.0855 (all data). Crystallographic data for the structural analysis has been deposited with the Cambridge Crystallographic Data Centre, CCDC No. 222749.

Acknowledgements

References

[1] S. Barlow, D. O'Hare, Chem. Rev. 97 (1997) 637.
[2] R.D.A. Hudson, J. Organomet. Chem. 637–639 (2001) 47.
[3] A. Hradsky, B. Bildstein, N. Schuler, H. Schottenberger, P. Jaitner, K.-H. Ongania, K. Wurst, J.-P. Launay, Organometallics 16 (1997) 392.
[4] H. Nishihara, Adv. Inorg. Chem. 53 (2002) 41.
[5] H. Nishihara, Bull. Chem. Soc. Jpn. 74 (2001) 19.
[6] M.R. Buchmeiser, A. Hallbrucker, I. Kohl, N. Schuler, H. Schottenberger, Des. Monomers Polym. 3 (2000) 421.
[7] R. Sanders, U.T. Mueller-Westerhoff, J. Organomet. Chem. 512 (1996) 219.
[8] E. Stankovic, S. Toma, R. Van Boxel, I. Asselberghs, A. Persoons, J. Organomet. Chem. 637–639 (2001) 426.
[9] R.H. Herber, I. Nowik, H. Schottenberger, K. Wurst, N. Schuler, A.G. Mueller, J. Organomet. Chem. 682 (2003) 163.
[10] B. Garrigues, Phosphorus Sulfur Silicon 53 (1990) 75.
[11] A.J. Bard, L.R. Faulkner, Electrochemical Methods; Fundamentals and Applications, second ed., Wiley, New York, Chichester, Brisbane, Toronto, 2001, p. 246.
[12] J.B. Flanagan, S. Margel, A.J. Bard, F.C. Anson, J. Am. Chem. Soc. 100 (1978) 4248.
[13] (a) D.H. Evans, M.W. Lehmann, Acta Chem. Scand. 53 (1999) 765;
(b) M.W. Lehmann, P. Singh, D.H. Evans, J. Electroanal. Chem. 549 (2003) 137;
(c) C. Kraiya, D.H. Evans, J. Electroanal. Chem. 565 (2004) 29.
[14] M. Can, K. Pekmez, N. Pekmez, A. Yildiz, Synth. Met. 104 (1999) 9.
[15] P. Audebert, L. Guyard, D.A. Nguyen, P. Hapiot, M. Chahma, C. Combelas, A. Thiebault, J. Electroanal. Chem. 407 (1996) 169.
[16] M. Sato, Y. Kawata, A. Kudo, A. Iwai, H. Saitoh, S. Ochiai, J. Chem. Soc., Dalton Trans. (1998) 2215.
[17] D. Obendorf, H. Schottenberger, C. Rieker, Organometallics 10 (1991) 1293.
[18] A.F. Diaz, U.T. Mueller-Westerhoff, A. Nazzal, M. Tanner, J. Organomet. Chem. 236 (1982) C45.
[19] D. Obendorf, C. Rieker, G. Ingram, J. Electroanal. Chem. 326 (1992) 81.
[20] J.C. Smart, B.L. Pinsky, J. Am. Chem. Soc. 99 (1977) 956.
[21] P.R. Sharp, K.N. Raymond, J.C. Smart, R.J. McKinney, J. Am. Chem. Soc. 103 (1981) 753.
[22] F. Barriere, N. Camire, W.E. Geiger, U.T. Mueller-Westerhoff, R. Sanders, J. Am. Chem. Soc. 124 (2002) 7262.
[23] H. Schottenberger, G. Ingram, D. Obendorf, J. Organomet. Chem. 426 (1992) 109.
[24] H. Schottenberger, G. Ingram, D. Obendorf, R. Tessadri, Synlett (1991) 905.
[25] I. Noviandri, K.N. Brown, D.S. Fleming, P.T. Gulyas, P.A. Lay, A.F. Masters, L. Phillips, J. Phys. Chem. B 103 (1999) 6713.
[26] A.J. Fry, W.E. Britton (Eds.), Topics in Organic Electrochemistry, Plenum, New York London, 1986.
[27] P. Jaitner, H. Schottenberger, S. Gamper, D. Obendorf, J. Organomet. Chem. 475 (1994) 113, and references cited.